

Preparation and magnetic properties of monodispersed Zn ferrites of submicrometric size

M. ANDRÉS-VERGÉS

Dpto. Química Inorgánica, Fac. Ciencias, Universidad Extremadura, Avda. Elvas s/n, 06071 Badajoz, Spain

C. de JULIÁN, J.M. GONZÁLEZ, C.J. SERNA

Instituto de Ciencia de Materiales–C.S.I.C., Serrano 115 dupl., 28006 Madrid, Spain

Mixed ferrite samples of the $Zn_xFe_{3-x}O_4$ system have been prepared by the solution method aiming at the obtention of submicrometric monodispersed particles. The crystalline structure, chemical composition and morphology of the samples was studied by means of X-ray diffraction, electron microscopy and energy-dispersive X-ray spectroscopy. The results obtained in this characterization evidenced (for samples of a given nominal composition) the uniformity in shape and size of the particles and their chemical homogeneity down to the particle level. Nevertheless, measurements of the specific magnetization of the samples suggest some degree of inhomogeneity in the intraparticle cationic distribution.

1. Introduction

Most ferrites are produced by conventional processing methods. Thus, metal oxides or carbonates are mixed, calcined and ground to produce fine ferrite powders which, nevertheless, result upon compacting (e.g. cold pressing) in non-ideal packing with a large porosity. As a consequence, high sintering temperatures are needed for densification in order to remove the larger pores within the particles [1].

An elegant solution to this problem is to prepare particles uniform in size and shape, i.e. monodispersed. This concept has been realized in practice for some ceramic systems which sinter to high densities at comparatively low temperatures [2, 3]. In the particular case of ferrites, two different approaches have been followed to prepare particles with spherical morphology: aerosol decomposition and solution methods.

The ferrite particles obtained by aerosol decomposition usually have the form of hollow spheres with a wide distribution in diameter [4, 5] and due to this reason solution methods are preferred and have been extensively used. Matijevic and co-workers [6, 7] have shown that spherical particles of Ni, Co and (Co, Ni) ferrite can be prepared from a solution containing Fe^{2+} by coprecipitation with controlled oxidation by nitrates. The ferrite particles obtained were in the form of spheres with a distribution of diameters ranging from 0.2 to 2 μm . Also, preparation of monodisperse Cr, Sr and Ba ferrite particles has been reported [8, 9].

From the standpoint of magnetic properties, a general problem concerning ferrite powders prepared by solution methods is the determination of the degree of chemical homogeneity inside the particles, since it would affect strongly their hysteretic behaviour [10].

Considering the above-mentioned systems, only Co ferrite particles have been shown to be totally homogeneous in composition whereas Ni, Cr, Sr and Ba ferrites have been established to be composed of inhomogeneous particles.

We have chosen the $Zn_xFe_{3-x}O_4$ system to determine the possibility of preparing, by means of the method reported for Co ferrites, [7] mixed ferrite powders composed of uniform spherical particles with homogeneous chemical composition. The magnetic properties of the system $Zn_xFe_{3-x}O_4$ have been previously reported by Miyata [11], measuring samples prepared by ceramic methods in which large chemical segregation was found within the particles.

2. Experimental procedure

2.1. Materials

All chemicals were reagent grade. The solutions were made up with doubly distilled water and passed through 0.22 μm Millipore filters to remove any particle contaminant. A stock solution of 0.5 M $FeSO_4$ was prepared by dissolving $FeSO_4 \cdot 7H_2O$ in 0.01 M H_2SO_4 under N_2 atmosphere to prevent the air oxidation of Fe^{2+} ion during storage.

2.2. Preparation of Zn ferrites

Zn ferrites ($Zn_xFe_{3-x}O_4$) were prepared by the so-called solution method [6–9] as follows. Nitrogen gas was bubbled through a solution containing 0.1 M KOH and $0.2\text{--}6.7 \times 10^{-3}$ M KNO_3 during several hours to eliminate the dissolved O_2 and CO_2 . It has been previously shown that when oxygen is present in

addition to nitrate ion, α -FeOOH particles crystallize along with ferrite during the ageing of ferrous hydroxide [12]. After that, different proportions of 0.5 M FeSO_4 and 0.5 M $\text{Zn}(\text{NO}_3)_2$ solutions (to vary the Zn/Fe atomic ratio from 0.5 ($x = 1$) to 0 ($x = 0$) and such that $[\text{M}]_{\text{total}} = 0.05 \text{ M}$) were introduced into the tightly closed system and with strong stirring. In all cases, the ratio of alkali to $[\text{Fe}^{2+}, \text{Zn}]$ was kept constant and equal to stoichiometric $\text{M}^{2+}[\text{OH}]_2$.

The reaction vessel containing the $(\text{Fe}, \text{Zn}) (\text{OH})_2$ precipitate was immersed in a constant-temperature bath preheated to 90°C and the system maintained with stirring for 24 h. Finally, the products were washed with water and dried at 60°C .

2.3. Characterization and magnetic measurements.

Structural and morphological characterization of the solids was carried out by X-ray diffraction, (XRD, Philips 1710), transmission electron microscopy, (TEM, Philips 300) and infrared spectroscopy, (Nico-

let 20SXC, KBr pellets). X-ray diffraction patterns were used to determine the phases present in samples with different nominal compositions. As a general rule characterization was completed only in samples with spinel structure. Particular attention was paid to the range going from 30 to 35° of 2θ , where the intense (1 3 0) reflections of goethite (α -FeOOH) and (1 0 4) of haematite (α - Fe_2O_3) can be observed. To determine the Zn/Fe atomic ratio, some samples were analysed by means of a scanning electron microscope (SEM, ISI DS-130) equipped with energy-dispersive X-ray analysis (EDX).

To perform the magnetic measurements, the original powders were pressed into a cylindrical shape (3 mm height, 3 mm diameter) using silver colloid as a binder. The packing factor obtained using a pressure of $2 \times 10^3 \text{ bar}$ was close to 0.5. The high-field specific magnetization of the samples was measured by means of an extraction device based on a superconducting coil using a maximum field of 2 T. The hysteretic behaviour at lower fields, and in particular the coercive force, was studied by means of a vibrating sample

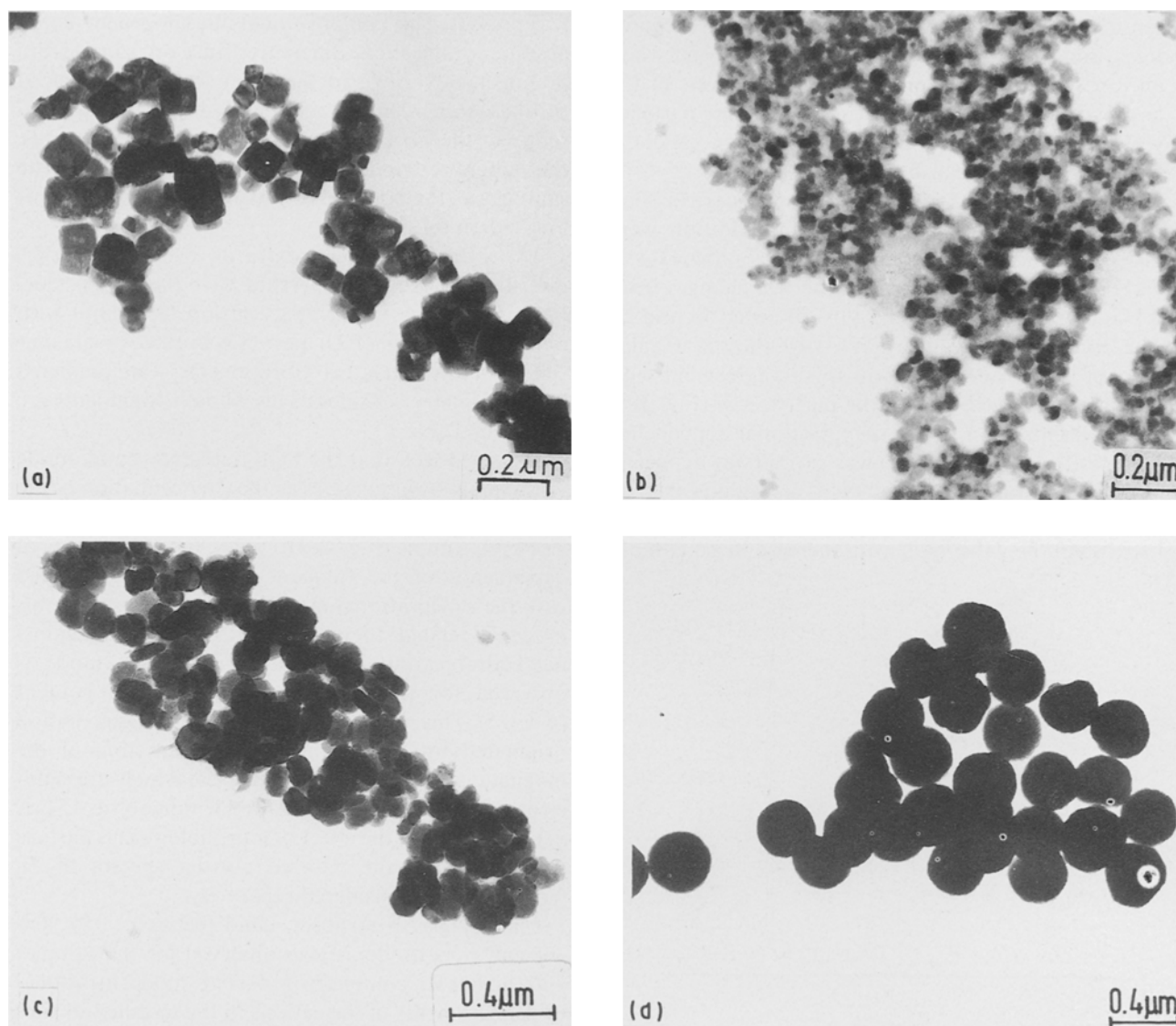


Figure 1 TEM micrographs of several Zn ferrites: (a) ZnFe_2O_4 , prepared using slow precipitation rate, (b) ZnFe_2O_4 , prepared using rapid precipitation rate, (c) $\text{Zn}_{0.5}\text{Fe}_{2.5}\text{O}_4$, (d) Fe_3O_4 (magnetite).

magnetometer based on an electromagnet (maximum field 0.7 T). In this case the samples were saturated in a 2 T field before the coercive force was measured.

3. Results and discussion

3.1. Preparation and crystallochemical characterization

As described in the experimental section, the preparation of Zn ferrites was carried out by coprecipitation of Fe^{2+} and Zn^{2+} hydroxides with subsequent ageing of the system at 90°C in the presence of an oxidant (KNO_3). Typical electron micrographs of the particles for different chemical compositions are shown in Fig. 1. Particles uniform in shape and size were observed irrespective of the nominal chemical composition, with a rather constant particle diameter of about $0.1\ \mu\text{m}$. Only for magnetite, $x = 0$, was the mean particle diameter larger, $\approx 0.3\ \mu\text{m}$ (Fig. 1d). It is worth pointing out that the morphology changes from cube-shaped ZnFe_2O_4 , $x = 1$, to spherical particles in the case of $\text{Fe}^{2+}\text{Fe}_2^{3+}\text{O}_4$, $x = 0$, i.e. as the substitution of Zn^{2+} by Fe^{2+} proceeds. For magnetite, the particle morphology has previously been found to depend on the concentration of the reacting components, in the sense that spherical particles are formed in an excess of Fe^{2+} and cubic-shaped particles are produced when an excess of KOH is present [12]. However, in Co ferrites an excess of hydroxide ions produces particles with poorly defined size and shape and an excess of Co broadens the size distribution [6].

On the other hand, variations in particle size associated with different rates of reactant addition were observed. This is illustrated in Fig. 1 for the case of ZnFe_2O_4 , where the mean particle size changes from 0.1 to $0.02\ \mu\text{m}$ by increasing this rate (Fig. 1a and b). The X-ray diffraction patterns also show a regular increase in the line-width which is in agreement with the differences observed in the particle size (Fig. 2).

A determination of the compositional dependence of the lattice parameter (a_0) was carried out by means of X-ray diffraction using TICL as standard. The results are plotted in Fig. 3, where a continuous increase in the value of a_0 with increase in Zn content

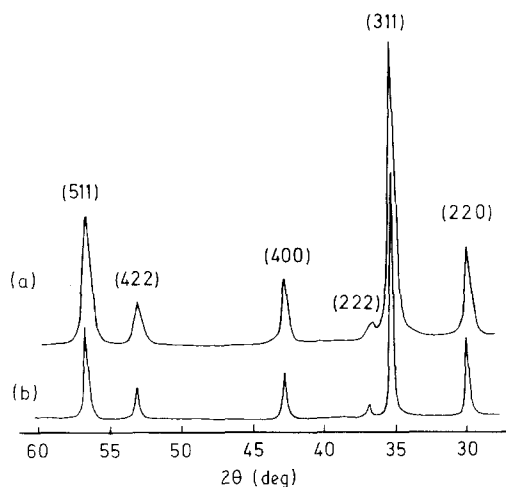


Figure 2 X-ray diffraction patterns measured in ZnFe_2O_4 samples prepared with (a) rapid precipitation rate, (b) slow precipitation rate.

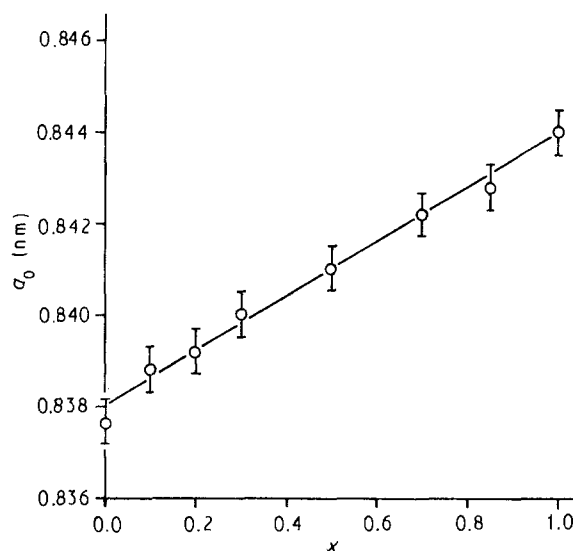


Figure 3 Compositional dependence of the lattice parameter in the $\text{Zn}_x\text{Fe}_{3-x}\text{O}_4$ system.

can be observed. The measured a_0 values were, for any composition, smaller than those reported by Miyata [11] for Zn ferrites prepared by solid-state reaction in which a large segregation in chemical composition was present. This compositional inhomogeneity could account for the above differences since our samples are homogeneous down to the $1\ \mu\text{m}$ scale, as evidenced through measurement by energy-dispersive spectroscopy of the Zn/Fe atomic ratio. In addition to this, the actual composition measured in each ferrite sample was the nominal one with standard deviations lower than 0.1.

The infrared powder spectra of several Zn ferrites are shown in Fig. 4. Zn ferrites have the spinel structure and belong to the space group $\text{O}_h^7(\text{Fd}3\text{m})$ with two formula units of $\text{Zn}_x\text{Fe}_{3-x}\text{O}_4$ in the Bravais unit cell. Four infrared lattice vibrations (F_{1u}) are predicted from symmetry considerations whose assignments are shown in Table 1.

It can be seen that the high-frequency band, mode ν_1 , shifts to lower energies as the Zn occupation of the tetrahedral sites increases, reaching $548\ \text{cm}^{-1}$ for the ZnFe_2O_4 sample (Fig. 4). However, the compositional dependence of the frequency maximum associated with the ν_2 vibrational mode is not so clear, since this mode is related to movements of oxygens against octahedral cations. A shoulder of the ν_2 mode is observed for the samples with lower Zn content ($x < 0.5$). This must be related to particle aggregation originated by the magnetostatic interaction of the magnetic moments of the particles, which are sufficiently large in this compositional range [14, 15]. A detailed study of the effect of morphology and particle aggregation on the infrared powder spectra of Zn ferrites will be considered separately.

Finally, an absorption band between 350 and $330\ \text{cm}^{-1}$, ν_3 mode, is also observed for the samples with higher Zn content (Fig. 4). This mode, attributed to displacements of the cations in the tetrahedral sites against the octahedral sites, becomes more evident as the structure evolves towards the normal spinel. In ZnFe_2O_4 ν_3 is clearly resolved at $330\ \text{cm}^{-1}$ (Fig. 4).

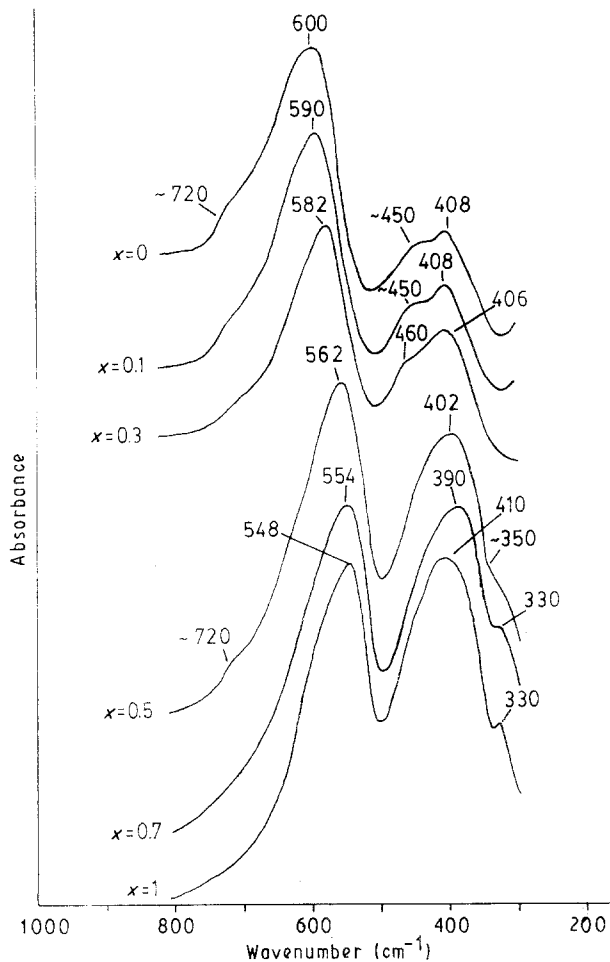


Figure 4 Infrared powder spectra for several compositions in the $Zn_xFe_{3-x}O_4$ system.

TABLE I Infrared absorption band assignments for Zn ferrites

Symmetry	Frequency range (cm^{-1})	Assignment [12]
$F_{1u}(\nu_1)$	600–548	M_T-O-M_O stretching
$F_{1u}(\nu_2)$	450–400	M_O-O stretching
$F_{1u}(\nu_3)$	350–330	M_T-M_O
$F_{1u}(\nu_4)$	< 200	M_T-M_T

3.2. Magnetic characterization

The magnetic characterization of the samples was centred on measurement of the specific saturation magnetization and the coercive force. It is worth pointing out that whereas the saturation magnetization is an intrinsic characteristic of the samples, the coercive force is very sensitive to the microstructure in the sense that it can be determined by a variety of factors including the shape and size of the particles.

As is well known [16], the saturation magnetization of ultrafine particles is usually lower than that measured in bulk samples of the same composition. In the particular case of $\gamma-Fe_2O_3$ particles this has been attributed [17] to a variation, on the surface of the particles, of the exchange interactions originating the ferrimagnetic ordering. This local variation produces an appreciable canting of the near-surface spins. Due to this reason and trying to minimize other spurious effects, the evaluation of the specific saturation magnetization σ_s was carried out by extrapolating to

infinite field the magnetic moment values measured in the range of applied fields from 1 up to 2 T.

In Fig. 5 we present, as a function of the composition, the specific saturation magnetization evaluated as explained above. An initial linear increase of the magnetization with the Zn content can be observed, which is associated with the progressive substitution of Fe^{3+} by Zn^{2+} in the tetrahedral sites (in equilibrium the Zn cations have a definite tendency to occupy only these sites) and to the consequent diminution of the number of Fe^{2+} cations per unit cell in the octahedral sites required by conservation of the electrical charge. The measured specific magnetization follows for the low Zn-containing samples the law

$$\sigma_s(x) = \sigma_s(0) + \alpha x$$

where $\sigma_s(0)$ is the magnetization of the magnetite and α takes a value of $98 \text{ A m}^2 \text{ kg}^{-1}$ which is consistent with the above-mentioned mechanism originating the increase in magnetization. The tendency of the magnetization to increase with increasing Zn content breaks down for Zn concentrations larger than $x = 0.2$. Above this value a progressive diminution of σ_s is observed which, nevertheless, leads to non-zero magnetization values for high Zn-containing samples and, particularly, to values in the range from 5 to $10 \text{ A m}^2 \text{ kg}^{-1}$ for pure Zn ferrite samples. This is not to be expected if one considers only the changes in the cationic distribution (which should originate a monotonic increase) and has been explained [18] by considering the compositional variations of the exchange interactions in the four sublattices (two tetrahedral and two octahedral) that are used to describe in detail the magnetic structure of these ferrites.

Actually, well-ordered pure Zn ferrite has been observed to be paramagnetic at room temperature and only indirect evidence of a Néel transition at very low temperatures has been published [19]. In this frame work we understand that the non-zero values we have obtained for the samples with the highest Zn content are related to a disorder in the cationic distribution with respect to the ideal one. More concretely, we propose, for the high Zn-containing particles, a structure consisting of two different zones: a core of almost stoichiometric $ZnFe_2O_4$ with a significant amount of Fe^{2+} still present in the octahedral sites, and an external shell with a cationic distribution

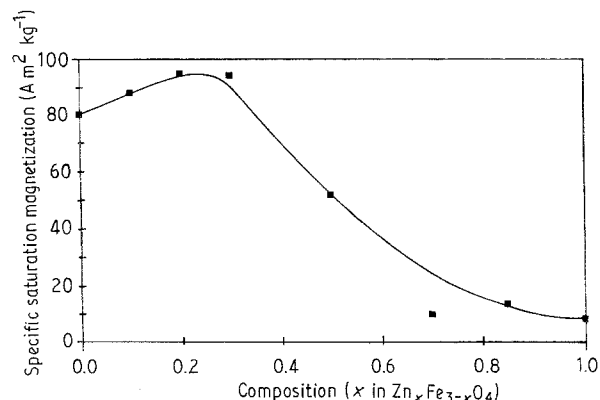


Figure 5 Compositional dependence of the specific saturation magnetization in the $Zn_xFe_{3-x}O_4$ system.

similar to that corresponding to a lower nominal Zn content (and in the limit similar to magnetite or to γ - Fe_2O_3 that could be produced by oxidation from magnetite). This type of microstructure has been previously proposed for small particles of ZnFe_2O_4 prepared by air oxidation of aqueous suspensions [20]. The external shell (ferrimagnetic or superparamagnetic depending on its dimensions) could be responsible for the residual magnetization measured in the as-obtained samples.

In order to test this idea we measured the magnetization of pure Zn ferrite samples prepared with different particle sizes (from a mean diameter of 140 nm down to 40 nm). Our results can be seen in Fig. 6 and, if the value of the magnetization of the samples is a measure of the disorder in the cationic distribution, we can observe that this disorder is maximum for the smaller particles and diminishes with an increase in particle size. Fig. 6 also presents the values of magnetization measured in this set of samples after annealing them under vacuum at 500 °C for 24 h. This thermal treatment was sufficient to make the magnetization decrease in all the samples to a value which was close to zero. It can then be concluded that after suitable thermal treatment, the cationic distribution can be relaxed to an equilibrium state leading, for this composition, to a paramagnetic behaviour.

Finally, in Fig. 7 we present the values of the coercive force H_c measured on the series. It is apparent that, with the sole exception of the samples with low

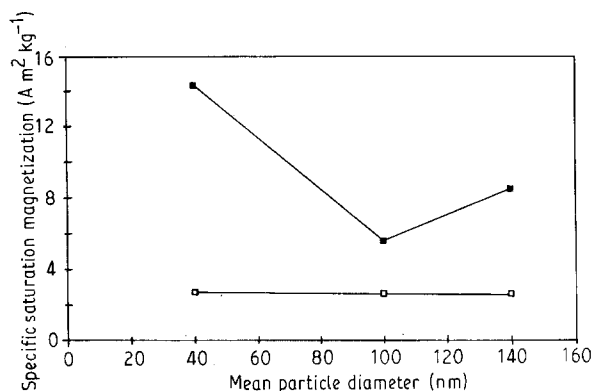


Figure 6 Specific magnetization values measured in ZnFe_2O_4 particles (■) as-prepared and (□) annealed under vacuum (500 °C, 24 h) as a function of their mean diameter.

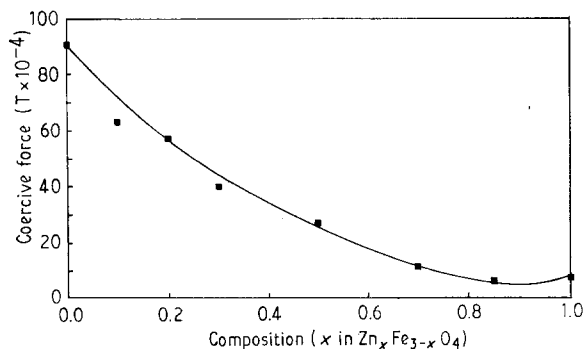


Figure 7 Compositional dependence of the coercive force in the $\text{Zn}_x\text{Fe}_{3-x}\text{O}_4$ system.

Zn content, the coercive force follows a compositional dependence which closely resembles that of specific saturation magnetization, thus showing the shape origin of the magnetic anisotropy ruling the magnetization process of the samples.

4. Conclusions

We have prepared mixed Zn ferrites by coprecipitation in solution. The particles so obtained are homogeneous in shape, size and chemical composition when examined by electron microscopy and energy-dispersive spectroscopy. Nevertheless, measurement of the compositional dependence of the specific magnetization evidences the presence of an out-of-equilibrium inhomogeneous cation distribution within the as-prepared particles. This cation distribution is relaxed to equilibrium by suitable thermal treatment.

Acknowledgements

We thank Dr V. García Martínez for his assistance with the electron microscope. The research was supported by the Spanish CICYT under projects MAT88-0201 and MAT91-0371.

References

1. D. W. JOHNSON Jr. and B. B. GHATE, in Proceedings of 4th International Conference on Ferrites, edited by F. F. Y. Wang, Advances in Ceramics Vol. 15 (The American Ceramic Society Inc, Columbus, Ohio, 1984) p. 27.
2. H. E. BOWEN. *Sci. Amer.* **255** (1986) 147.
3. M. OCAÑA, V. FORNÉS and C. J. SERNA. *Ceram. Inter.* **18** (1992) 99.
4. A. M. GADALLA and H. F. YU. *J. Mater. Res.* **5** (1990) 2923.
5. T. GONZÁLEZ-CARREÑO, A. MIFSUD, C. J. SERNA and J. M. PALACIOS, *Mater. Chem. Phys.* **27** (1991) 278.
6. A. E. RAGAZZONI and E. MATIJEVIC. *Colloids Surf.* **6** (1983) 189.
7. H. TAMURA and E. MATIJEVIC. *Colloids Interf. Sci.* **90** (1982) 100.
8. E. MATIJEVIC, C. M. SIMPSON, N. AMIN and S. ARAIS. *Colloids Surf.* **21** (1986) 101.
9. E. MATIJEVIC. *J. Colloid Interf. Sci.* **117** (1987) 593.
10. J. SMIT and J. WIJN, in "Ferrites" (Paraninfo, Madrid, 1965) p. 150.
11. N. MIYATA. *J. Phys. Soc. Jpn* **16** (1961) 1291.
12. T. SUGIMOTO and E. MATIJEVIC. *J. Colloid Interf. Sci.* **74** (1980) 227.
13. V. C. FARMER, in "The Infrared Spectra of Minerals", edited by V. C. Farmer (Mineralogical Society, London, 1974) p. 183.
14. C. J. SERNA, M. OCAÑA and J. E. IGLESIAS. *J. Phys. C* **20** (1987) 473.
15. J. E. IGLESIAS, M. OCAÑA and C. J. SERNA. *Appl. Spectrosc.* **44** (1990) 418.
16. A. E. BERKOWITZ, W. J. SCHUELE and P. J. FLANDERS. *J. Appl. Phys.* **39** (1968) 1261.
17. J. M. D. COEY. *Phys. Rev. Lett.* **27** (1971) 1140.
18. J. SMIT and J. WIJN in "Ferrites" (Madrid, 1965) p. 178.
19. P. I. SLICK in "Ferromagnetic Materials" edited by E. P. Wohlforth (North Holland, Amsterdam, 1980) p. 201.
20. M. KIYAMA and T. TAKADA, in Proceedings of ICF 3, Kyoto, 1980, p. 11, edited by H. Watanabe, S. Iida and M. Sugimoto (Center for Academic Publications, Tokyo, 1981).

Received 10 April
and accepted 11 August 1992